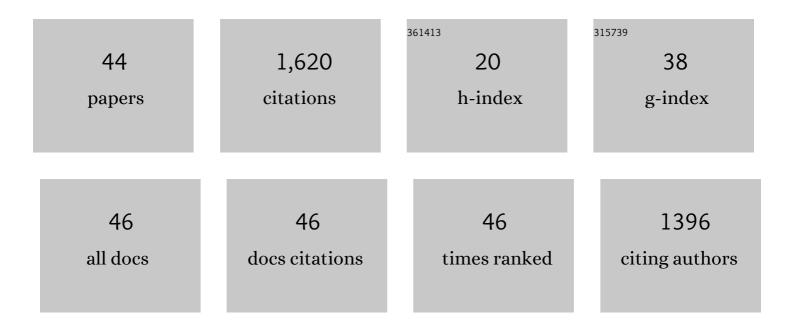
Stephan Walrand

List of Publications by Year in descending order

Source: https://exaly.com/author-pdf/2452197/publications.pdf Version: 2024-02-01



#	Article	IF	CITATIONS
1	Optimization of the Clinical Effectiveness of Radioembolization in Hepatocellular Carcinoma with Dosimetry and Patient-Selection Criteria. Current Oncology, 2022, 29, 2422-2434.	2.2	2
2	Direct effect of the Directive Euratom 2013/59 on European hospitals hosting radionuclide therapies. Physica Medica, 2022, 96, 121-122.	0.7	1
3	Bremsstrahlung SPECT/CT. , 2022, , 293-303.		Ο
4	TCP post-radioembolization and TCP post-EBRT in HCC are similar and can be predicted using the in vitro radiosensitivity. EJNMMI Research, 2022, 12, .	2.5	2
5	Autumn COVID-19 surge dates in Europe correlated to latitudes, not to temperature-humidity, pointing to vitamin D as contributing factor. Scientific Reports, 2021, 11, 1981.	3.3	40
6	Hepatic Arterial Buffer Response in Liver Radioembolization and Potential Use for Improved Cancer Therapy. Cancers, 2021, 13, 1537.	3.7	5
7	Prediction of tumor response and patient outcome after radioembolization of hepatocellular carcinoma using 90Y-PET-computed tomography dosimetry. Nuclear Medicine Communications, 2021, 42, 747-754.	1.1	9
8	Microspheres Used in Liver Radioembolization: From Conception to Clinical Effects. Molecules, 2021, 26, 3966.	3.8	29
9	Renal and Red Marrow Dosimetry in Peptide Receptor Radionuclide Therapy: 20 Years of History and Ahead. International Journal of Molecular Sciences, 2021, 22, 8326.	4.1	7
10	Accurate non-tumoral 99mTc-MAA absorbed dose prediction to plan optimized activities in liver radioembolization using resin microspheres. Physica Medica, 2021, 89, 250-257.	0.7	11
11	Yttrium-90 TOF-PET-Based EUD Predicts Response Post Liver Radioembolizations Using Recommended Manufacturer FDG Reconstruction Parameters. Frontiers in Oncology, 2021, 11, 592529.	2.8	7
12	Antireflux catheter improves tumor targeting in liver radioembolization with resin microspheres. , 2021, 27, 768-773.		8
13	EANM dosimetry committee series on standard operational procedures: a unified methodology for 99mTc-MAA pre- and 90Y peri-therapy dosimetry in liver radioembolization with 90Y microspheres. EJNMMI Physics, 2021, 8, 77.	2.7	61
14	Achieving sub-100 ps time-of-flight resolution in thick LSO positron emission tomography while reducing system cost: a Monte Carlo study. Physics in Medicine and Biology, 2020, 65, 205009.	3.0	2
15	Re: Tumor Targeting and Three-Dimensional Voxel-Based Dosimetry to Predict Tumor Response, Toxicity, and Survival after Yttrium-90 Resin Microsphere Radioembolization in Hepatocellular Carcinoma. Journal of Vascular and Interventional Radiology, 2019, 30, 2047-2048.	0.5	3
16	Significant artefactual noise in 90Y TOF-PET imaging of low specific activity phantoms arises despite increased acquisition time. EJNMMI Physics, 2019, 6, 20.	2.7	2
17	The origin and reduction of spurious extrahepatic counts observed in ⁹⁰ Y non-TOF PET imaging post radioembolization. Physics in Medicine and Biology, 2018, 63, 075016.	3.0	8
18	Update on novel trends in PET/CT technology and its clinical applications. British Journal of Radiology, 2018, 91, 20160534.	2.2	18

STEPHAN WALRAND

#	Article	IF	CITATIONS
19	Biodistribution of 125I-labeled anti-endoglin antibody using SPECT/CT imaging: Impact of in vivo deiodination on tumor accumulation in mice. Nuclear Medicine and Biology, 2016, 43, 415-423.	0.6	13
20	Statistical and radiobiological analysis of the so-called thyroid stunning. EJNMMI Research, 2015, 5, 67.	2.5	17
21	The Impact of Image Reconstruction Bias on PET/CT ⁹⁰ Y Dosimetry After Radioembolization. Journal of Nuclear Medicine, 2015, 56, 494.2-495.	5.0	2
22	Optimal Design of Anger Camera for Bremsstrahlung Imaging: Monte Carlo Evaluation. Frontiers in Oncology, 2014, 4, 149.	2.8	15
23	The role of SPECT/CT in radioembolization of liver tumours. European Journal of Nuclear Medicine and Molecular Imaging, 2014, 41, 115-124.	6.4	38
24	A Hepatic Dose-Toxicity Model Opening the Way Toward Individualized Radioembolization Planning. Journal of Nuclear Medicine, 2014, 55, 1317-1322.	5.0	44
25	The Low Hepatic Toxicity per Gray of ⁹⁰ Y Glass Microspheres Is Linked to Their Transport in the Arterial Tree Favoring a Nonuniform Trapping as Observed in Posttherapy PET Imaging. Journal of Nuclear Medicine, 2014, 55, 135-140.	5.0	75
26	Bremsstrahlung SPECT/CT. , 2014, , 271-280.		1
27	SPECT/CT for Dosimetry. , 2014, , 29-42.		0
28	Perspectives in Nuclear Medicine Tomography: A Physicist's Point of View. , 2013, , 69-96.		2
29	Tumour control probability derived from dose distribution in homogeneous and heterogeneous models: assuming similar pharmacokinetics, ¹²⁵ Sn– ¹⁷⁷ Lu is superior to ⁹⁰ Y– ¹⁷⁷ Lu in peptide receptor radiotherapy. Physics in Medicine and Biology, 2012, 57, 4263-4275.	3.0	16
30	Hemoglobin level significantly impacts the tumor cell survival fraction in humans after internal radiotherapy. EJNMMI Research, 2012, 2, 20.	2.5	31
31	Comparison of yttrium-90 quantitative imaging by TOF and non-TOF PET in a phantom of liver selective internal radiotherapy. Physics in Medicine and Biology, 2011, 56, 6759-6777.	3.0	48
32	Yttrium-90-labeled microsphere tracking during liver selective internal radiotherapy by bremsstrahlung pinhole SPECT: feasibility study and evaluation in an abdominal phantom. EJNMMI Research, 2011, 1, 32.	2.5	36
33	Experimental facts supporting a red marrow uptake due to radiometal transchelation in 90Y-DOTATOC therapy and relationship to the decrease of platelet counts. European Journal of Nuclear Medicine and Molecular Imaging, 2011, 38, 1270-1280.	6.4	59
34	Dosimetry of yttrium-labelled radiopharmaceuticals for internal therapy: 86Y or 90Y imaging?. European Journal of Nuclear Medicine and Molecular Imaging, 2011, 38, 57-68.	6.4	79
35	Is bone marrow uptake of 86Y-DOTATOC routinely observed?. European Journal of Nuclear Medicine and Molecular Imaging, 2011, 38, 1742-1743.	6.4	0
36	Feasibility of 90Y TOF PET-based dosimetry in liver metastasis therapy using SIR-Spheres. European Journal of Nuclear Medicine and Molecular Imaging, 2010, 37, 1654-1662.	6.4	177

STEPHAN WALRAND

#	Article	IF	CITATIONS
37	4-Step Renal Dosimetry Dependent on Cortex Geometry Applied to ⁹⁰ Y Peptide Receptor Radiotherapy: Evaluation Using a Fillable Kidney Phantom Imaged by ⁹⁰ Y PET. Journal of Nuclear Medicine, 2010, 51, 1969-1973.	5.0	37
38	Yttrium-90 TOF PET scan demonstrates high-resolution biodistribution after liver SIRT. European Journal of Nuclear Medicine and Molecular Imaging, 2009, 36, 1696-1696.	6.4	139
39	Practical dosimetry of peptide receptor radionuclide therapy with (90)Y-labeled somatostatin analogs. Journal of Nuclear Medicine, 2005, 46 Suppl 1, 92S-8S.	5.0	60
40	Patient-specific dosimetry in predicting renal toxicity with (90)Y-DOTATOC: relevance of kidney volume and dose rate in finding a dose-effect relationship. Journal of Nuclear Medicine, 2005, 46 Suppl 1, 99S-106S.	5.0	107
41	Megalin is essential for renal proximal tubule reabsorption of (111)In-DTPA-octreotide. Journal of Nuclear Medicine, 2005, 46, 1696-700.	5.0	73
42	Evaluation of novel whole-body high-resolution rodent SPECT (Linoview) based on direct acquisition of linogram projections. Journal of Nuclear Medicine, 2005, 46, 1872-80.	5.0	42
43	Quantitation in PET using isotopes emitting prompt single gammas: application to yttrium-86. European Journal of Nuclear Medicine and Molecular Imaging, 2003, 30, 354-361.	6.4	81
44	86Y-DOTA0-d-Phe1-Tyr3-octreotide (SMT487)—a phase 1 clinical study: pharmacokinetics, biodistribution and renal protective effect of different regimens of amino acid co-infusion. European Journal of Nuclear Medicine and Molecular Imaging, 2003, 30, 510-518.	6.4	212

Nuclear Medicine and Molecular Imaging, 2003, 30, 510-518.